Journal of the Meteorological Society of Japan, Vol. 81, No. 2, pp. 277–293, 2003

Regionalization of Surface Fluxes over Heterogeneous Landscape of the Tibetan Plateau by Using Satellite Remote Sensing Data

Yaoming MA

Cold and Arid Regions Environmental and Engineering Research Institute, Chinese Academy of Sciences, Lanzhou, China
Institute of Tibetan Plateau Research, Chinese Academy of Sciences, Beijing, China

Hirohiko ISHIKAWA

Disaster Prevention Research Institute, Kyoto University, Kyoto, Japan

Osamu TSUKAMOTO

Faculty of Sciences, Okayama University, Okayama, Japan

Massimo MENENTI, Zhongbo SU

Alterra Green World Research, Wageningen, The Netherlands

Tandong YAO

Cold and Arid Regions Environmental and Engineering Research Institute, Chinese Academy of Sciences, Lanzhou, China
Institute of Tibetan Plateau Research, Chinese Academy of Sciences, Beijing, China

Toshio KOIKE

Department of Civil Engineering, University of Tokyo, Tokyo, Japan

and

Tetsuzo YASUNARI

Institute of Geoscience, University of Tsukuba, Tsukuba, Japan

(Manuscript received 29 March 2002, in revised form 9 December 2002)

Corresponding author: Yaoming Ma, Department of Plateau Atmospheric Physics, Cold and Arid Regions Environmental and Engineering Research Institute (CAREERI), Chinese Academy of Sciences (CAS), 260 Dong-gang West Road, Lanzhou, Gansu 730000, China.
E-mail: ymma@ns.lzb.ac.cn

Abstract

In this study, a parameterization method based on NOAA-14/AVHRR data and field observations is described and tested for deriving the regional land surface variables, vegetation variables and land surface heat fluxes over a heterogeneous landscape. As a case study, the method was applied to the Tibetan Plateau area. The regional distribution maps of surface reflectance, MSAVI, vegetation coverage, surface temperature, net radiation, soil heat flux, sensible heat flux and latent heat flux were determined over the Tibetan Plateau area. The derived results were validated by using the "ground truth". The results show that the more reasonable regional distributions and their seasonal variations of land surface variables (surface reflectance, surface temperature), vegetation variables (MSAVI and vegetation coverage), net radiation, soil heat flux and sensible heat flux can be obtained by using the method proposed in this study. However, the approach of deriving regional latent heat flux, and their seasonal variation as the residual of the energy budget, may not be a good method due to the unbalance of energy and the strong advection over the study area. Further improvement of the method was also discussed.

1. Introduction

The Tibetan Plateau, with one million km^2 area and the averaged altitude of about 4000 m, plays a very important role in the Asian monsoon circulation, and the global climate change. The GEWEX Asian Monsoon Experiment over the Tibetan Plateau, GAME-Tibet, was carried out in the Tibetan Plateau, and the intensive observation period (IOP) was continued from May to September 1998. The experimental region, about 100×200 km^2, includes a variety of land surfaces such as a large area of grassy marshland, some arid areas, many small rivers and several lakes. At different landscapes, two basic comprehensive observation stations (Anduo and NaquFx), two Flux-PAM (Portable Automated Meso-net) observation stations (MS3478-NPAM and MS3637-SPAM), three automatic weather stations (D110-AWS110, Naqu and MS3608-AWS3608), one 3D Doppler Radar, radio sonde system, soil moisture and soil temperature net, rain gauge net and barometer net had been operated continuously for almost five months. A large amount of surface observation data has been collected (Fig. 1).

The study on the energy exchanges between the land surface and atmosphere was of paramount importance for GAME-Tibet. Some interesting detailed studies concerning the land surface heat fluxes have been reported (Ishikawa et al. 1999; Tamagawa et al. 1999; Tsukamoto et al. 1999; Wang et al. 1999; Ma et al. 1999a; Ma et al. 1999c; Yasunari 1999; Kuwagata et al. 1999; Ma et al. 2000; Koike 2000; Tanaka et al. 2001). These researches were, however, on point-level or a local-patch-level. Since the aerial, but not only point-wise, information of land-surface atmosphere interaction is required, the aggregation of the individual results into a regional scale is necessary. Remote sensing from satellites offers the possibility to derive regional distribution of land surface heat fluxes.

The purpose of this study is to upscale the point or patch scale field observations of land surface variables, and land surface heat fluxes to meso-scale distribution of them with the aid of NOAA-14/AVHRR data. First describe the methodology in section 2. The application of the methodology to the GAME/Tibet period is presented in section 3, where the distribution of land surface variables, vegetation variables, and land surface heat fluxes are estimated for three different phases, pre-monsoon, mid-monsoon, and post-monsoon. Discussions are also given in the section.

2. Data and methodology

2.1 Data

The NOAA-14 Advanced Very High Resolution Radiometer (AVHRR) provides spectral information in 5 bands, with a spatial resolution of about 1 km $\times$ 1 km. Three scenes of satellite data used in this study were collected at 14:43 h (Local Time at 92°E, LT) June 12, 1998, 13:21 h (LT) 16 July, 1998 and 13:25 h (LT), August 21, 1998.

The most relevant field data, collected at the GAME/Tibet surface stations, consists of radiosounding, vertical profiles of air temperature, wind speed and humidity, soil heat flux, surface

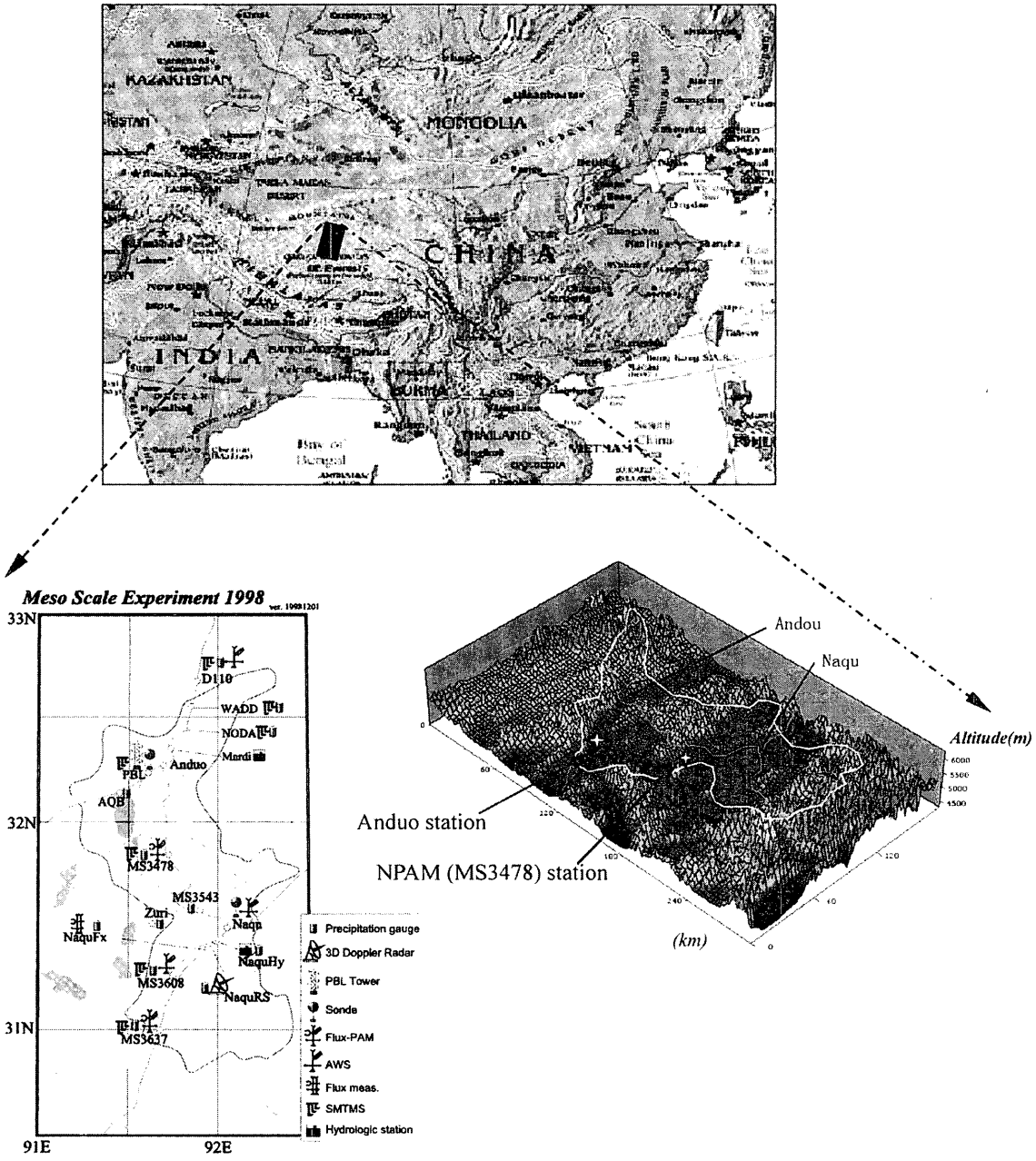

Fig. 1. The geographic map and the sites layout during IOP of the GAME/Tibet.

radiation budget components, turbulent fluxes measured by eddy-correlation technique and PBL tower, and the vegetation state.

2.2 *Methodology*

The general concept of the methodology is shown in a diagram (Fig. 2). The surface reflectance for short-wave radiation (r_0), and land surface temperature (T_{sfc}), are retrieved from NOAA-14/AVHRR data with the atmospheric correction by radiative transfer model MODTRAN (Berk et al. 1989) using aero-logical observation data. The radiative transfer model also computes the downward short- and long-wave radiation at the surface. With these results the surface net radiation (R_n) is deter-

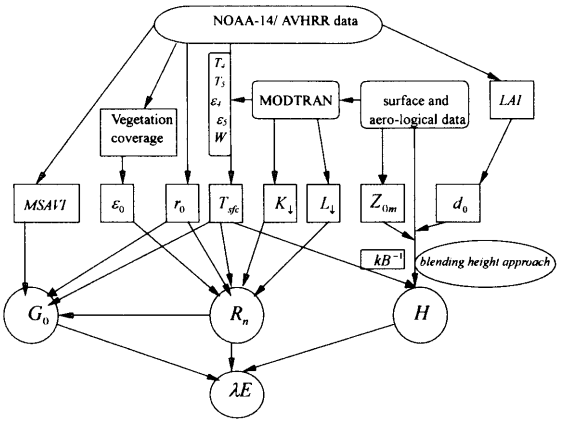

Fig. 2. Diagram of parameterization procedure combining NOAA-14/AVHRR data with field observations.

mined. The soil heat flux (G_0) is estimated from R_n, T_{sfc}, r_0 and MSAVI (Modified Soil Adjusted Vegetation Index, Qi et al. 1994) which is also derived from NOAA-14/AVHRR data. The sensible heat flux (H) is estimated from T_{sfc}, surface and aero-logical data with the aid of so called 'blending height' approach (Mason 1988).

a. Net radiation

The regional net radiation flux is expressed as

$$R_n(x,y) = (1 - r_0(x,y)) \cdot K_{\downarrow}(x,y) + L_{\downarrow}(x,y) - \varepsilon_0(x,y)\sigma T_{sfc}^4(x,y), \quad (1)$$

where surface reflectance $r_0(x,y)$ is derived from the channel-1 and -2 of NOAA-14/AVHRR data with the models of Paltridge and Mithchell (1990) and Valiente et al. (1995). The surface emissivity $\varepsilon_0(x,y)$ is a function of vegetation coverage, and the vegetation coverage P_v is also derived from channel 1 and 2 data with the algorithm by Valor and Caselles (1996), i.e.,

$$P_v(x,y) = \frac{1 - \dfrac{NDVI(x,y)}{NDVI_s}}{\left[1 - \dfrac{NDVI(x,y)}{NDVI_s}\right] - K\left[1 - \dfrac{NDVI(x,y)}{NDVI_v}\right]}, \quad (2)$$

where $K = (r_{2v} - r_{1v})/(r_{2g} - r_{1g})$, which r_{2v}, r_{1v} and r_{2g}, r_{1g} are the minimum and maximum reflectance value of AVHRR channel-2 and channel-1. $NDVI_s$ and $NDVI_v$ are the NDVI values for bare soil and full vegetation respectively.

The land surface temperature $T_{sfc}(x,y)$ in Eq. (1) is retrieved from the brightness temperature of channels four and five of NOAA-14/AVHRR according to Becker and Li (1990 and 1995). We first assume that the T_{sfc} is expressed as

$$T_{sfc} = F(T_4, T_5, \varepsilon_4, \varepsilon_5, W, \theta), \quad (3)$$

where T_4 and T_5 are the brightness temperatures of channels 4 and 5 of AVHRR, ε_4 and ε_5 are the spectral emissivities of channel 4 and 5 respectively, W is water vapor content, which can be derived from MODTRAN (Kneizys et al. 1996) model by using air temperature and humidity profiles observed through the radio sonde, and θ represents the view angle of satellite. Equation (3) was expressed by different split window algorithms (Becker and Li 1995). The algorithm proposed by Sobrino and Raissouni (2000) will be used in this study, i.e.,

$$T_{sfc}(x,y) = T_4(x,y) + 1.40[T_4(x,y) - T_5(x,y)] + 0.28[T_4(x,y) - T_5(x,y)]^2 + 0.83 + (57 - 5W)(1 - \varepsilon) - (161 - 30W)\Delta\varepsilon, \quad (4)$$

where $\varepsilon = (\varepsilon_4 + \varepsilon_5)/2$, $\Delta\varepsilon = \varepsilon_4 - \varepsilon_5$ (Li and Becker 1993).

The incoming short-wave radiation flux $K_{\downarrow}(x,y)$ in Eq. (1) could be derived from radiative transfer model MODTRAN (Kneizys et al. 1996), where atmospheric short-wave transmittance τ_{sw} is obtained by using the radio sonde data and the surface reflectance and surface temperature observed in the field. Hence $K_{\downarrow}(x,y)$ can be obtained as

$$K_{\downarrow}(x,y) = \tau_{sw} K_{TOA}^{\downarrow}(x,y), \quad (5)$$

where the regional variation of radiation flux perpendicular to the top of atmosphere $K_{TOA}^{\downarrow}(x,y)$ is a spectrally integrated form of in-band radiation flux perpendicular to the top of atmosphere $K_{TOA}^{\downarrow}(\lambda)$, and

$$K_{TOA}^{\downarrow}(x,y) = \frac{K_{exo}^{\downarrow}(b)\cos\theta_{sun}(x,y)}{d_s^2}, \quad (6)$$

where $K_{exo}^{\downarrow}(b)$ is the averaged in-band solar exo-atmospheric irradiance undisturbed by θ_{sun} be-

ing zero, b is abbreviation of in-band, d_s is the earth-sun distance, θ_{sun} is sun zenith angle. The incoming long-wave radiation flux $L_{\downarrow}(x, y)$ in Eq. (1) could also be calculated from MODTRAN by using the radio sonde data and the surface reflectance and surface temperature observed in the field.

b. Soil heat flux

The regional soil heat flux $G_0(x, y)$ is usually determined by (Choudhury and Monteith 1988)

$$G_0(x, y) = \rho_s C_s[(T_{sfc}(x, y) - T_s(x, y)]/r_{sh}(x, y), \tag{7}$$

where ρ_s is soil dry bulk density, C_s is soil specific heat, $T_s(x, y)$ stands for soil temperature of a determined depth, $r_{sh}(x, y)$ represents soil heat transportation resistance. However, the regional soil heat flux $G_0(x, y)$ cannot directly be mapped from satellite observations through Equation (7) for the difficulty to determine the soil heat transportation resistance $r_{sh}(x, y)$, and the soil temperature at a reference depth $T_s(x, y)$. Many investigations have shown that the mid-day G_0/R_n fraction is reasonably predicted from special vegetation indices (Daughtry et al. 1990). Some researchers have shown that $G_0/R_n = \Gamma(NDVI)$ (Clothier et al. 1986; Choudhury et al. 1987; Kustas and Daughtry 1990). An improved fraction of $G_0/R_n = \Gamma(r_0, T_{sfc}, NDVI)$ was proposed (Menenti et al. 1991; Bastiaanssen 1995). However, problems exist in the NDVI definition equation because of the effects of external factors, such as soil background variations (Huete et al. 1985; Huete 1989). In order to reduce the soil background effect in NDVI, a parameterization based on MSAVI is proposed over the Tibetan area in this study as

$$\begin{aligned} G_0(x, y) = {} & R_n(x, y) \cdot (T_{sfc}(x, y)/r_0(x, y)) \\ & \cdot (a + b\bar{r}_0 + c\bar{r}_0^2) \\ & \cdot [1 + dMSAVI(x, y)^e], \end{aligned} \tag{8}$$

where the constants a, b, c, d and e are determined by using the field data observed at six observation stations (AWS110, Anduo, NPAM, Naqu, AWS3608 and SPAM) during the GAME/Tibet IOP; $\bar{r}_0$ is a daily mean reflectance value obtained from field observations. $MSAVI(x, y)$ was derived from the band reflectance of channel 1 and 2 of NOAA-14/AVHRR as (Qi et al. 1994)

$$MSAVI(x, y) = \frac{2r_2(x, y) + 1 - \sqrt{[2r_2(x, y) + 1]^2 - 8[r_2(x, y) - r_1(x, y)]}}{2}. \tag{9}$$

c. Sensible and latent heat fluxes

The sensible heat flux $H(x, y)$ can be derived from

$$H(x, y) = \rho C_P \frac{T_{sfc}(x, y) - T_a(x, y)}{r_a(x, y)}, \tag{10}$$

where aerodynamic resistance $r_a(x, y)$ is

$$r_a(x, y) = \frac{1}{ku_*(x, y)} \times \left[\ln\left(\frac{z - d_0(x, y)}{Z_{0m}(x, y)}\right) + kB^{-1}(x, y) - \psi_h(x, y)\right], \tag{11}$$

and

$$u_*(x, y) = ku(x, y)\left[\ln\left(\frac{z - d_0(x, y)}{Z_{0m}(x, y)}\right) - \psi_m(x, y)\right]^{-1}, \tag{12}$$

where k is the Von-Karman constant, u_* is the friction velocity, z is reference height, d_0 is zero-plane displacement height, Z_{0m} is the effective aerodynamic roughness, ψ_m and ψ_h are the stability correction function, and kB^{-1} is the excess resistance to heat transfer, and (Owen and Thomson 1963; Chamberlain 1968)

$$kB^{-1} = \ln\left(\frac{z_{0m}}{z_{0h}}\right), \tag{13}$$

where z_{0m} and z_{0h} are aerodynamic roughness and thermodynamic roughness, respectively.

Combining Eqs. (10), (11) and (12) yields

$$H(x, y) = \rho C_P k^2 u(x, y) \times \frac{[T_{sfc}(x, y) - T_a(x, y)]}{\left[\ln\frac{z - d_0(x, y)}{Z_{0m}(x, y)} + kB^{-1}(x, y) - \psi_h(x, y)\right] \cdot \left[\ln\frac{z - d_0(x, y)}{Z_{0m}(x, y)} - \psi_m(x, y)\right]}. \tag{14}$$

The straightforward way to model sensible heat flux in a large area is to sum up the contribution from different surface elements. If the local scale advection is comparatively small, it is desired that the development of a convective

boundary layer may smooth the local heterogeneity of surface disorganized variety at the so called 'blending height', where atmospheric characteristics become proximately independent of horizontal locations. The corresponding 'effective' surface variables can be determined accordingly (Mason 1988). This approach has been proved to be successful to calculate regional averaged surface fluxes recently (Lhomme et al. 1994; Bastiaassen 1995; Wang et al. 1995; Ma et al. 1999b; Ma et al. 2002b). Based on this approach, the regional sensible heat flux $H(x, y)$ is expressed as

$$H(x, y) = \rho C_P k^2 u_B \times \frac{[T_{sfc}(x, y) - T_{air\text{-}B}]}{\left[\ln\frac{Z_B - d_0(x, y)}{Z_{0m}(x, y)} + kB^{-1}(x, y) - \psi_h(x, y)\right] \cdot \left[\ln\frac{Z_B - d_0(x, y)}{Z_{0m}(x, y)} - \psi_m(x, y)\right]}, \quad (15)$$

where Z_B is the blending height, u_B and $T_{air\text{-}B}$ are wind speed and air temperature at the blending height respectively. Z_B, u_B and $T_{air\text{-}B}$ are determined by using field measurements or numerical models. In this study, these variables will be determined with the aid of field measurements of radio sonde. $Z_{0m}(x, y)$ is the effective aerodynamic roughness length including the effect of topography and low vegetation (e.g., grass), and is determined by the Taylor's model (Taylor et al. 1989). The excess resistance to heat transfer, kB^{-1}, is shown as a function of surface temperature over the Tibetan Plateau area (Ma et al. 2002a). d_0 is zero-plane displacement, which can be calculated from Raupach's model (Raupach 1994) over this area. $\psi_h(x, y)$ and $\psi_m(x, y)$ are the integrated stability functions in equation (15). For unstable condition, the integrated stability functions $\psi_h(x, y)$ and $\psi_m(x, y)$ are written as (Paulson 1970)

$$\begin{cases} \psi_m(x, y) = 2\ln\left(\dfrac{1+X}{2}\right) + \ln\left(\dfrac{1+X^2}{2}\right) - 2\arctan(X) + 0.5\pi, \\ \psi_h(x, y) = 2\ln\left(\dfrac{1+X^2}{2}\right), \end{cases} \quad (16)$$

where $X = \{1 - 16 * [z - d_0(x, y)]/L(x, y)\}^{0.25}$ and Monin Obukhov stability length $L = -kgH/(T_a u_*^3 \rho C_P)$. For stable condition, the integrated stability function $\psi_h(x, y)$ and $\psi_m(x, y)$ become (Webb 1970)

$$\psi_m(x, y) = \psi_h(x, y) = -5\frac{z - d_0(x, y)}{L(x, y)}. \quad (17)$$

The stability function $[z - d_0(x, y)]/L(x, y)$ will be solved by using the Businger scheme (Businger 1988), i.e.,

$$\begin{cases} \dfrac{z - d_0(x, y)}{L(x, y)} = R_i(x, y) \quad \text{(unstable)}, \\ \dfrac{z - d_0(x, y)}{L(x, y)} = R_i(x, y)/[1 - 5.2R_i(x, y)] \quad \text{(stable)}, \end{cases} \quad (18)$$

where $R_i(x, y)$ is the Richardson number.

The regional latent heat flux $\lambda E(x, y)$ is the residual of the energy budget theorem for land surface, i.e.,

$$\lambda E(x, y) = R_n(x, y) - H(x, y) - G_0(x, y). \quad (19)$$

3. Results and discussions

It is better to select the satellite data in clear days to study the distribution of land surface variables, vegetation variables and the energy budget components. Unfortunately, it was difficult to select this kind of satellite data over the Tibetan Plateau area for the strong convective clouds when NOAA-14/AVHRR observation took place. Only three scenes of the NOAA-14/AVHRR could be selected during the whole IOP. The scene of June 12, 1998 was selected as a case of pre-monsoon and whole mesoscale area. The scenes of July 16, 1998 and August 21, 1998 were selected as the cases of mid-monsoon and the post-monsoon. The images around Anduo station and NPAM station were selected as the comparable areas because fluxes measurements using sonic anemometer-thermometer were undertook at these two stations. It is also very clear around these two stations on the images of NOAA-14/AVHRR.

Figure 3 shows the distribution maps of surface reflectance, surface temperature, vegetation coverage, MSAVI and surface heat fluxes of the mesoscale experimental area. Each pixel is 1×1 km^2 and 180 by 51 pixels are shown. Figure 4 shows their frequency distribution of these variables over the whole mesoscale experimental area. The distribution of land surface variables and vegetation variables around Anduo station and NPAM station were compared for different phases of the monsoon in Fig. 5. The distribution of land surface heat

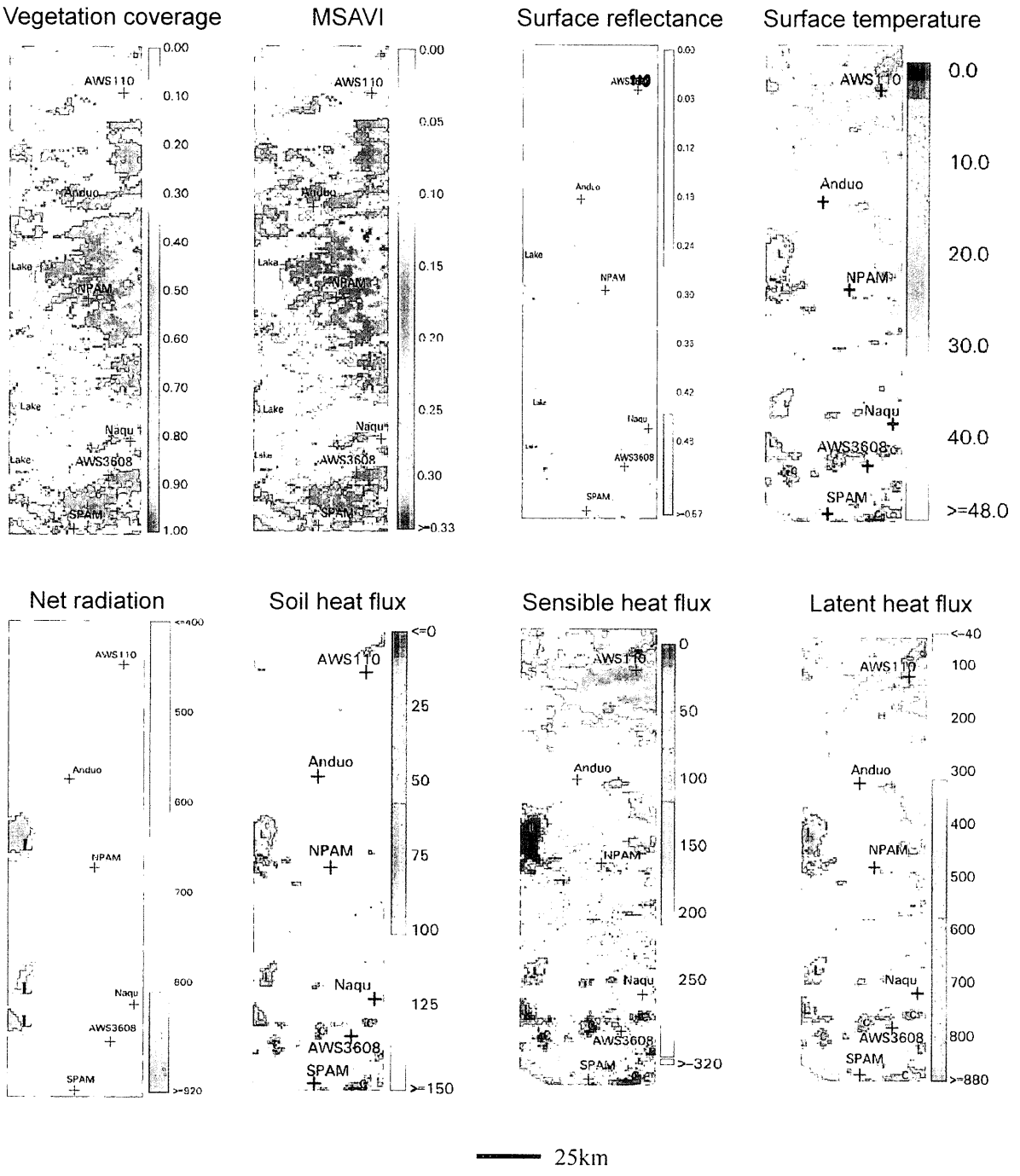

Fig. 3. The distribution maps of land surface variables, vegetation variables and land surface heat fluxes in June 12, 1998 for the GAME/Tibet area.

fluxes around Anduo station and NPAM station were also compared in Fig. 6. Both Fig. 5 and Fig. 6 are based on 45 by 40 pixels with a size of 1×1 km^2.

The land surface variables and land surface heat fluxes derived from satellite data were compared with the field measurements at Anduo and NPAM sites. They are shown in Fig. 7

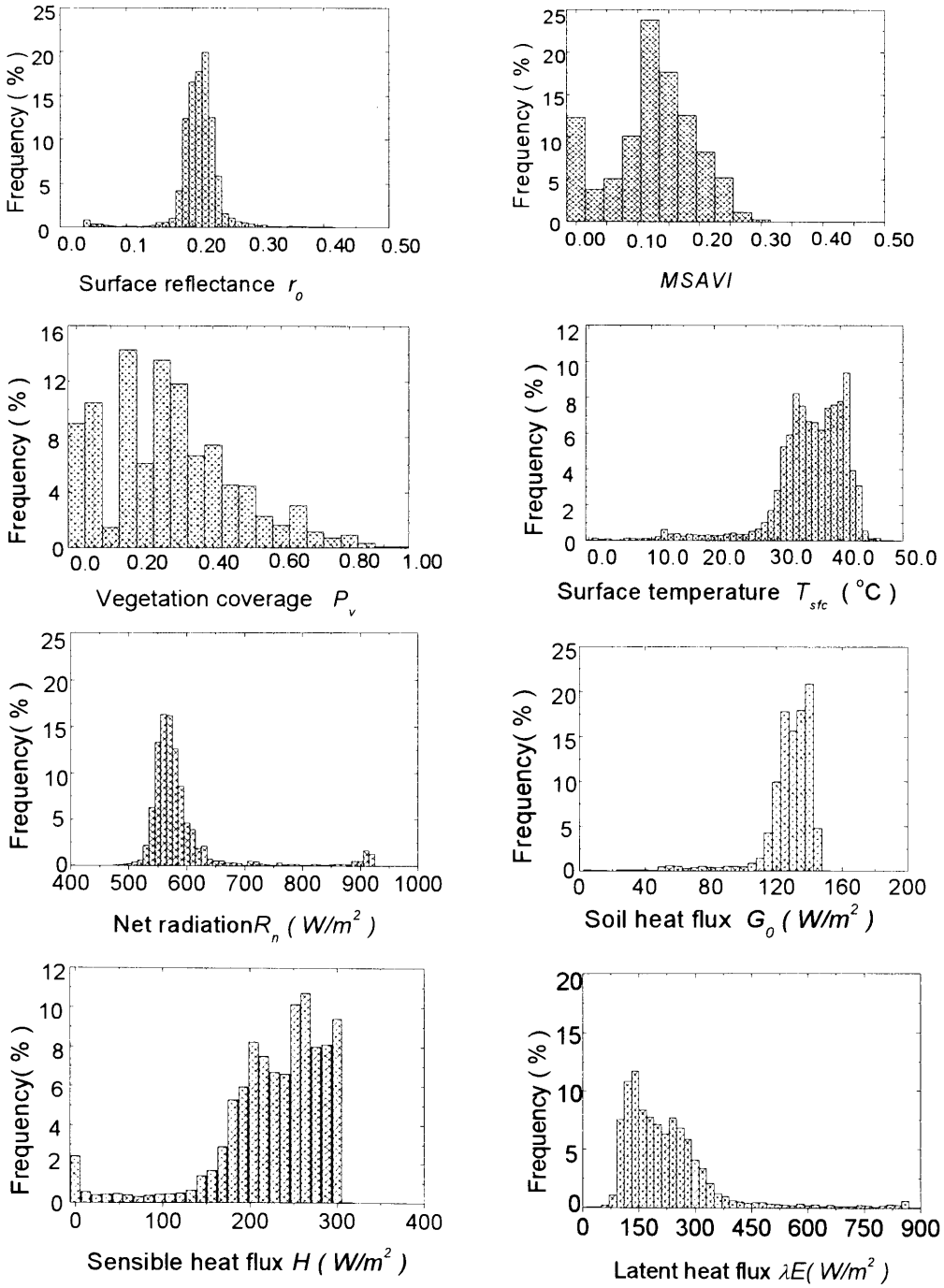

Fig. 4. The frequency distribution of land surface variables, vegetation variables, and land surface heat fluxes for the GAME/Tibet area. (June 12, 1998).

and Table 1. The field observational data, which used for validation here, was just measured at the time of satellite over passed the area, or ten minutes averaging value around that time. The mean absolute percent difference (MAPD) was computed as a quantitative measure of the difference between the derived results on No. i point ($H_{derived(i)}$), and mea-

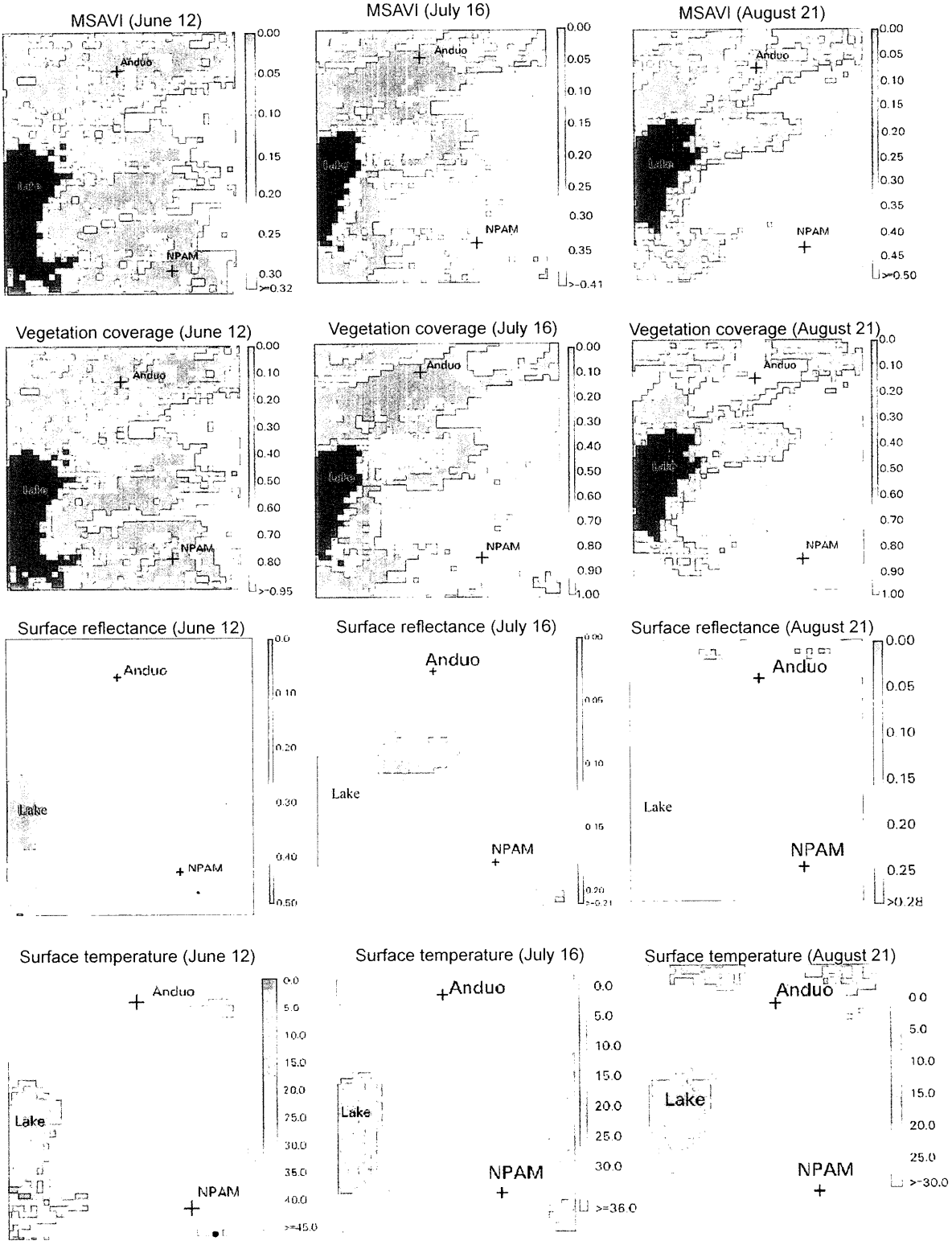

Fig. 5. The distribution maps of land variables and vegetation variables for the Tibetan Plateau area.

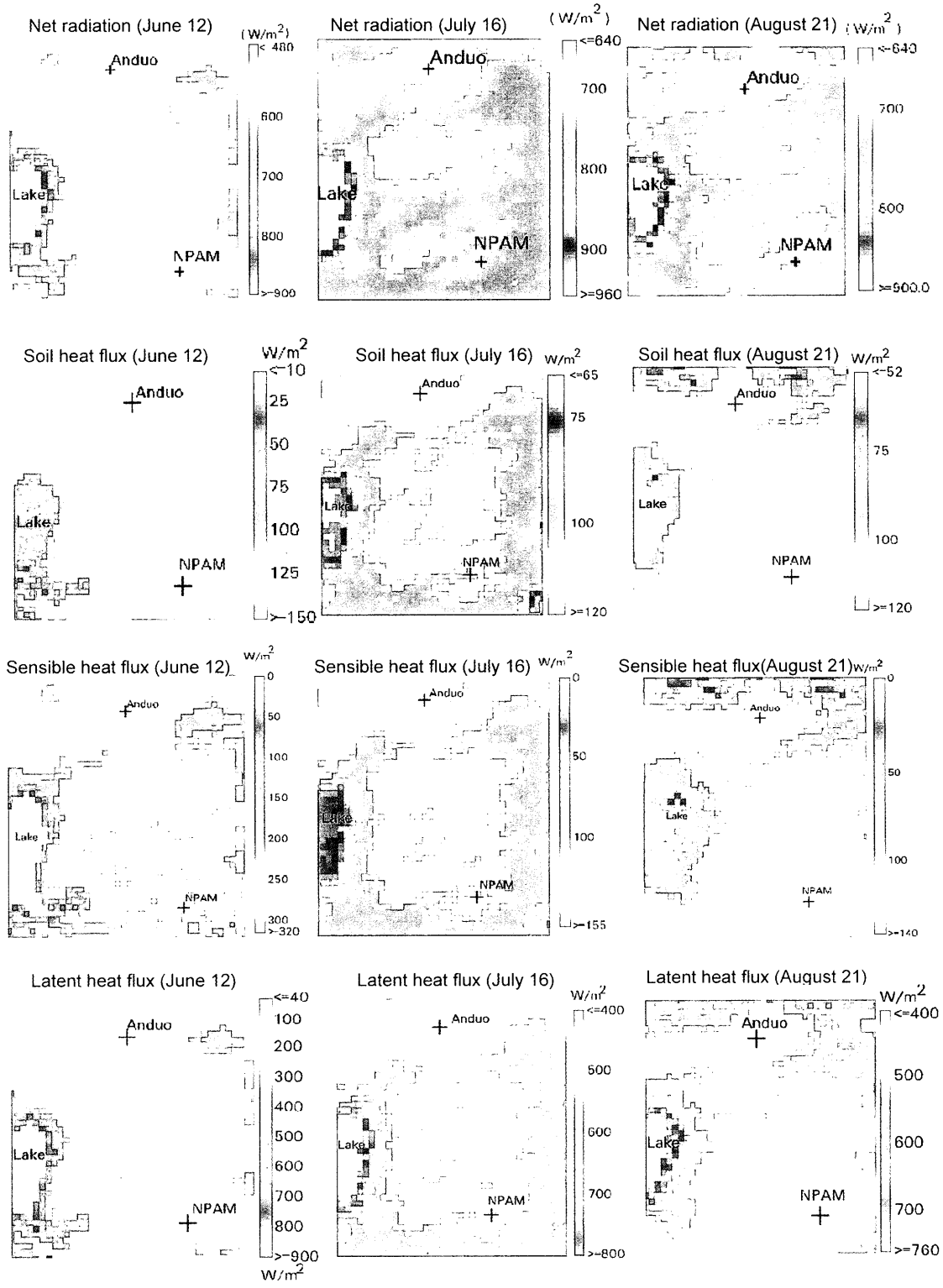

Fig. 6. The distribution maps of land surface heat fluxes for the Tibetan Plateau area.

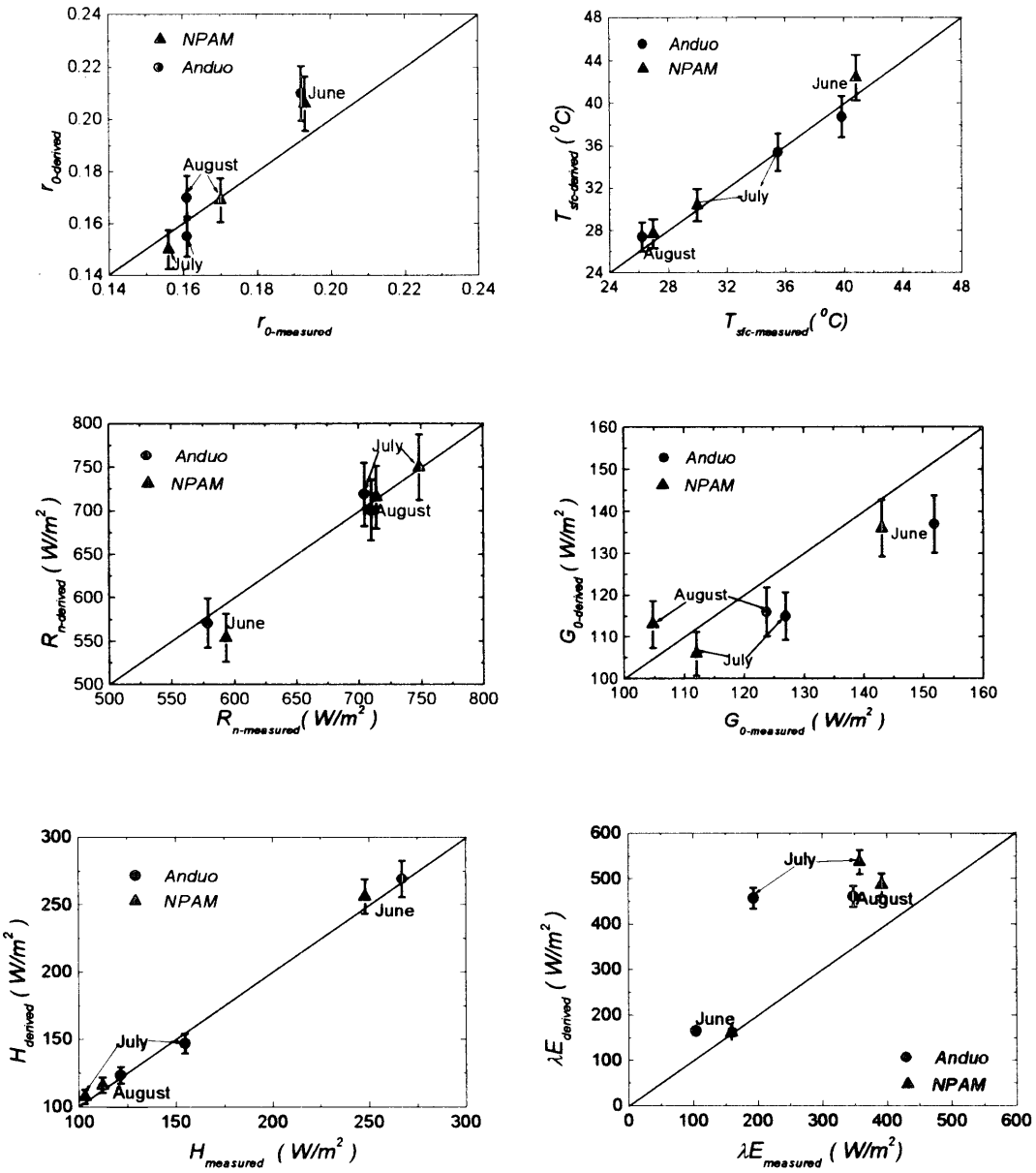

Fig. 7. Comparison of the derived results with the field measurements for the surface reflectance, surface temperature and land surface heat fluxes over the GAME/Tibet area, together with 1:1 line.

sured value on No. i point ($H_{measured(i)}$) of one scene as

$$MAPD = \frac{100}{n}\sum_{i=1}^{n}\left(\frac{|H_{derived(i)} - H_{measured(i)}|}{H_{measured(i)}}\right). \quad (20)$$

It is seen that: (1) the derived land surface variables, vegetation variables and heat fluxes for the whole meaoscale area on 12 June 1998 were in good accordance with the land surface status. These parameters show a wide range of variations due to the strong contrast of surface features in the study area. MSAVI varies from 0.00 to 0.30. Vegetation coverage P_v varies from 0.00 to 1.00. Surface reflectance is from 0.00 to 0.35 (some of the surface reflectance with value large than 0.35 indicating cloud-

Table 1. Comparison of the derived results (Cal.) versus those measured values (Meas.) at the GAME/Tibet site with *MAPD*

	r_0 (-)								
	June			July			August		
	Cal.	*Meas.*	*MAPD*	*Cal.*	*Meas.*	*MAPD*	*Cal.*	*Meas.*	*MAPD*
Anduo	0.208	0.192	8.33%	0.155	0.161	3.73%	0.170	0.161	5.59%
NPAM	0.206	0.193	6.73%	0.150	0.156	3.85%	0.172	0.173	0.59%
	T_{sfc} (^{0}C)								
	June			July			August		
	Cal.	*Meas.*	*MAPD*	*Cal.*	*Meas.*	*MAPD*	*Cal.*	*Meas.*	*MAPD*
Anduo	38.70	39.82	2.81%	35.56	35.48	0.23%	27.19	26.02	4.50%
NPAM	42.39	40.80	3.90%	30.40	29.98	1.40%	27.57	26.85	2.67%
	R_n (W m^{-2})								
	June			July			August		
	Cal.	*Meas.*	*MAPD*	*Cal.*	*Meas.*	*MAPD*	*Cal.*	*Meas.*	*MAPD*
Anduo	571.04	578.62	1.31%	714.95	700.11	2.12%	700.98	709.57	1.21%
NPAM	554.04	593.00	6.57%	749.99	748.27	0.23%	715.98	713.98	0.28%
	G_0 (W m^{-2})								
	June			July			August		
	Cal.$_{(MSAVI)}$	*Meas.*	*MAPD*	*Cal.*$_{(MSAVI)}$	*Meas.*	*MAPD*	*Cal.*$_{(MSAVI)}$	*Meas.*	*MAPD*
Anduo	136.58	151.32	9.74%	114.90	126.78	9.37%	116.00	123.76	6.27%
NPAM	135.39	142.46	4.96%	105.61	112.09	5.78%	113.36	105.11	7.85%
	Cal.$_{(NDVI)}$	*Meas.*	*MAPD*	*Cal.*$_{(NDVI)}$	*Meas.*	*MAPD*	*Cal.*$_{(NDVI)}$	*Meas.*	*MAPD*
Anduo	134.72	151.32	10.97%	110.87	126.78	12.55%	112.08	123.76	9.44%
NPAM	131.43	142.46	7.74%	101.45	112.09	9.49%	116.79	105.11	11.11%
	H (W m^{-2})								
	June			July			August		
	Cal.	*Meas.*	*MAPD*	*Cal.*	*Meas.*	*MAPD*	*Cal.*	*Meas.*	*MAPD*
Anduo	268.99	267.09	0.71%	147.01	154.76	5.01%	123.50	121.41	1.72%
NPAM	256.09	247.98	3.27%	107.50	102.94	4.43%	116.00	112.10	3.48%
	λE (W m^{-2})								
	June			July			August		
	Cal.	*Meas.*	*MAPD*	*Cal.*	*Meas.*	*MAPD*	*Cal.*	*Meas.*	*MAPD*
Anduo	165.47	101.05	63.75%	453.04	193.03	134.70%	461.48	347.87	32.66%
NPAM	162.56	159.45	1.95%	536.88	357.62	50.13%	486.62	391.57	24.27%

covering). Surface temperature ranged from 5°C to 48°C (surface temperature of 0.0°C indicating cloud-covering). Net radiation changed from 400 to 920 W/m^2. Soil heat flux varied from 0 to 150 W/m^2. Sensible heat flux is from 0 to 320 W/m^2, and latent heat flux varies from 40 to 880 W/m^2 (see Fig. 1, Fig. 3 and Fig. 4); (2) not only on June 12, but also on July 16 and August 21, the derived surface reflectance, surface temperature, net radiation flux, soil heat flux and sensible heat flux were close to the field measurements. The difference between the derived results and the field observation MAPD was less than 10% (see Table 2, Fig. 5, Fig. 6, Fig. 7 and MASVI case in the Table 1); (3) not only on June 12, but also on July 16 and August 2, the value of the vegetation coverage in this area was almost the same due to the land surface in this area is covered by the same grassy marshland in these days. The only difference was that the grass was dry on June 12 (with small MSAVI). It became green and wet on July 16 and August 21 (with higher MSAVI) for this area (see Fig. 5 and Fig. 6); (4) during the experimental periods, the derived net radiation flux was larger than that in the HEIFE area (Ma et al. 1999) due to the high altitude (the higher value of downward short-wave radiation), and land surface coverage of grassy marshland (the lower value of the upward long-wave radiation) in this area (see Fig. 3, Fig. 5 and Fig. 6). For example, the regional average value of net radiation flux was 470 W/m^2 over the HEIFE area in 9 July, 1991 and that was 750 W/m^2 over the GAME/Tibet area in 16 July, 1998; (5) the values of surface reflectance, surface temperature, soil heat flux and sensible heat flux in June over this area were larger than these values in July and August. Net radiation flux and latent heat flux in June were lower than their values in July and August. The reason is that June 12 was the day before the Asia Monsoon coming. The land surface was dry in that day. July 16 and August 21 were within and after the Asia Monsoon. The land surface was wet, and the grass was high and growing (see Fig. 3, Fig. 5 and Fig. 6); (6) problems existed in the NDVI definition equation because of the external factor effect, such as soil background variations (Huete et al. 1985; Huete 1989). To reduce the soil background effect, Qi et al. (1994) proposed using MSAVI. Therefore, the parameterization method based on MSAVI for soil heat flux is better than that based on NDVI on heterogeneous land surface of the Tibetan Plateau. The derived regional soil heat fluxes, based on MSAVI were reasonable in different months in this area with MAPD less than 10% (see Fig. 3, Fig. 6, Fig. 7 and Table 1), and it was better than the derived regional soil heat fluxes based on NDVI (see Table 1); and, (7) all elements of heat balance equation at NPAM site on June 12 well corresponded to the satellite data. On the other hand, all but latent heat flux corresponded to the satellite data in other seasons, and other stations. The conclusions derived from above facts were, (a) net radiation, sensible heat flux, and soil heat flux could be derived from satellite, (b) in the case of NPAM on June 12, because the surface energy balanced in the surface observation so that the latent heat flux estimated by surface observation, well corresponded to that estimated by the residual of satellite data analysis. One dimensional energy budget did not balance due to large errors of the latent heat flux through the surface observation and advection in this area. The large error of the measurement on latent heat flux may dpend on the accuracy of the turbulence measurement sensors (Ma et al. 1999a; Ishikawa et al. 1999; Wang et al. 1999; Ma et al. 1999c; Ma et al. 2000; Tanaka et al. 2001). This point and conclusion (a) clearly show the disagreement of latent heat flux between surface observations and satellite one.

4. Concluding remarks

In this study, distributions of land surface variables (surface reflectance and surface temperature), vegetation variables (MSAVI and vegetation coverage P_v), land surface heat fluxes (net radiation, soil heat flux and sensible heat flux) over the heterogeneous area of GAME/Tibet were derived by using NOAA-14/AVHRR data and field observations. The results were in good agreement with field observations. The approach of deriving regional latent heat flux, and their seasonal variation as the residual of the energy budget, may not be a good method due to one-dimensional energy budget unbalance and the strong advection over the study area when the satellite passed over the area. Future improvements are to

Table 2. List of symbols in this paper

Symbol	Interpretation	Unit
C_p	Air specific heat at constant pressure	J kg^{-1} K^{-1}
C_s	Soil specific heat	J kg^{-1} K^{-1}
d_0	Zero-plane displacement	m
d_s	Earth-Sun distance	AU
E	Evaporation flux	Kg m^{-2} s^{-1}
G_0	Soil heat flux	W m^{-2}
H	Sensible heat flux	W m^{-2}
k	Von Karman constant	-
kB^{-1}	Excess resistance to heat transfer	-
$K_{\downarrow}$	Incoming short-wave radiation flux	W m^{-2}
$K^{\downarrow}_{exo(b)}$	Mean in-band solar exo-atmospheric irradiance	W m^{-2}
$K^{\downarrow}_{TOA}$	Radiation flux perpendicular to the top of atmosphere	W m^{-2}
$K^{\downarrow}_{TOA(\lambda)}$	Bi-directional spectral radiance at the satellite sensor	W m^{-2} sr^{-1} μm^{-1}
L	Monin Obukhov stability length	m
$L_{\downarrow}$	Incoming long-wave radiation flux	W m^{-2}
$MSAVI$	Modified soil adjusted vegetation index	-
$NDVI$	Normalized Difference Vegetation Index	-
$NDVI_s$	NDVI values for bare soil	-
$NDVI_v$	NDVI value for full vegetation	-
r_0	Surface reflectance (surface albedo)	-
r_1	Band reflectance of channel 1 of NOAA/AVHRR	-
r_2	Band reflectance of channel 2 of NOAA/AVHRR	-
r_{2v}, r_{1v}	Minimum reflectance value of AVHRR channel-2 and channel-1	-
r_{2g}, r_{1g}	Maximum reflectance value of AVHRR channel-2 and channel-1	
r_a	Aerodynamic resistance	S m^{-1}
R_i	Richardson number	-
R_n	Net radiation flux	W m^{-2}
r_{sh}	Soil heat transportation resistance	S m^{-1}
T_a	Air temperature	K
$T_{air\text{-}B}$	Air temperature at the blending height	K
T_s	Soil temperature	K
T_{sfc}	Surface temperature	K
T_4	Brightness temperature of channel 4 of NOAA/AVHRR	K
T_5	Brightness temperature of channel 5 of NOAA/AVHRR	K
ε_0	Surface emissivity	-
ε_4	Spectral emissivity of channel 4 on NOAA/AVHRR	-
ε_5	Spectral emissivity of channel 5 on NOAA/AVHRR	-
u	Horizontal component of wind speed	m s^{-1}
u_B	Wind speed at the blending height	m s^{-1}
u_*	Friction velocity	m s^{-1}
W	Water vapor content	g m^{-3}
z	Reference height	m
z_{oh}	Thermodynamic roughness length	m
z_{om}	Aerodynamic roughness length	m
Z_{om}	Effective aerodynamic roughness length	m
z_B	Blending height	m
σ	Stefan Boltzmann constant	W m^{-2} K^{-4}
θ	View angle of satellite	degree
θ_{sun}	Sun zenith angle	rad
λ	Latent heat of vaporization	J kg^{-1}
λE	Latent heat flux	W m^{-2}
ρ	Air density	kg m^{-3}
ρ_s	Soil bulk density	kg m^{-3}
τ_{sw}	Atmospheric short-wave transmittance	-
ψ_h	Stability correction for atmospheric heat transport	-
ψ_m	Stability correction for atmospheric momentum transport	-

be made to derive more accurate regional latent heat flux over such areas. The advection $\partial S(x,y)/\partial t$ and the errors in the procedure of determining regional net radiation, soil heat flux and sensible heat flux $\Delta R_n(x,y)$, $\Delta G_0(x,y)$ and $\Delta H(x,y)$ will be considered in the equation of surface energy balance over this area, e.g.,

$$\lambda E(x,y) = R_n(x,y) + \Delta R_n(x,y) - [H(x,y) + \Delta H(x,y)] - [G_0(x,y) + \Delta G_0(x,y)] - \partial S(x,y)/\partial t. \quad (21)$$

In other words, the regional latent heat flux will be correctly derived when the advection $\partial S(x,y)/\partial t$ and the errors $\Delta R_n(x,y)$, $\Delta G_0(x,y)$ and $\Delta H(x,y)$ are determined by using the suitable models and much better measurement sensors.

It is also worth trying SEBI (Surface Energy Balance Index, Menenti and Choudhury 1993) method, which is based on the Penmen-Monteith equation (Monteith 1965).

Acknowledgement

The data used in this paper was obtained by the GAME-Tibet project supported by the Ministry of Education, Science, Sport and Culture of Japan; the Science and Technology Agency of Japan; the Chinese Academy of Science (CAS); the National Space Development Agency of Japan, and the Frontier Research System for Global Change. This research is under the auspices of National Science Foundation of China under Project No. 40275003, the Chinese National Key Project (G1998040900), the Innovation Project of the Chinese Academy of Science (KZCX2-301) and the Innovation project of Cold and Arid Regions Environmental and Engineering Research Institute, CAS (CACX210072). The first author would also like to acknowledge Dr. Zhaoliang Li for his very kindly help in the procedure of determining surface temperature, Prof. J. Wang, Dr. K. Ueno and Dr. J. Wen for their help in the procedure of the paper. The authors thank all the participants from China and Japan in the field observation. We are also grateful to the referees for their very useful comments and helpful suggestions, which contributed to the final version of the manuscript.

References

Bastiaanssen, W.G.M., 1995: Regionalization of surface fluxes and moisture indicators in composite terrain, *PhD Thesis*, Wageningen Agricultural University, 273pp.

Becker, F. and Zh. Li, 1990: Towards a local split window method over land surfaces, *Int. J. of Remote Sensing*, **11**(3), 369–393.

——— and ———, 1995: Surface temperature and emissivity at various scales: definition, measurement and related problems, *Remote Sensing Review*, **12**, 225–253.

Berk, A., L.S. Bernstein and D.C. Robertson, MODTRAN, 1989: A moderate resolution model for LOTRAN 7, GL-TR-89-0122.

Businger, J.A., 1988: A note on the Businger-Dyer profiles, *Bound.-Layer Meteor.*, **42**, 145–151.

Chamberlain, A.C., 1968: Transport of gases to and from surfaces with bluff and wave-like roughness elements, *Quart. J. Roy. Meteor. Soc.*, **94**, 318–332.

Choudhury, B.J. and J.L. Monteith, 1988: A four-layer model for the heat budget of homogeneous land surfaces, *Quart. J. Roy. Meteor. Soc.*, **114**, 373–398.

———, S.B. Idso and R.J. Reginato, 1987: Analysis of an empirical model for soil heat flux under a growing wheat crop for estimating evaporation by infrared-temperature based energy balance equation, *Agric. For. Meteor.*, **39**, 283–297.

Clothier, B.E., K.L. Clawson, P.J. Pinter, M.S. Moran, R.J. Reginato and R.D. Jackson, 1986: Estimating of soil heat flux from net radiation during the growth of alfalfa, *Agric. For. Meteor.*, **37**, 319–329.

Daughtry, C.S.T., W.P. Kustas, M.S. Moran, P.J. Pinter, R.D. Jackson, P.W. Brown, W.D. Nichols and L.W. Gay, 1990: Spectral estimates of net radiation and soil heat flux, *Remote Sens. Environ.*, **32**, 111–124.

Huete, A.R., R.D. Jackson and D.F. Post, 1985: Spectral response of a plant canopy with different soil backgrounds, *Remote Sens. Environ.*, **17**, 37–53.

———, 1989: Soil influences in remotely sensed vegetation-canopy spectra. *Theory and Applications of Optical Remote Sensing* (G. Asrar, Ed.), 107–141.

Ishikawa, H., O. Tsukamoto, T. Hayashi, I. Tamagawa, S. Miyazaki, J. Asanuma, Y. Qi, H. Fudeyasu and K. Tanaka, 1999: Summary of the boundary layer observation and the preliminary analysis, *Third International Scientific Conference on the Global Energy and Water Cycle*, Beijing, China, 16–19 June 1999, 45–459.

Kenizys, F.X., L.W. Abreu, G.P. Anderson, J.H. Chetwynd, E.P. Shettle, A. Berk, L.S. Bernstein, D.C. Robertson, P. Acharya, L.S. Rothman, J.E.A. Selby, W.O. Gallery and S.A. Clough, 1996: *The MODTRAN3/2 report and LODTRAN 7 Model.* (L.W. Abreu and G.P. Andson, Eds), prepared by Ontar Corp., North Andover, MA, for Phillips Laboratory, Geophysical Directorate, Hanscom AFB, MA., Contract No. F19628-91-C-0132.

Koike, T., 2000: The overview of GAME/Tibet, *The Second Session of International Workshop on TIPEX-GAME / TIBET*, Kunming, China, July 20–22.

Kustas, W.P. and C.S.T. Daughtry, 1990: Estimation of the soil heat flux/net radiation ratio from spectral data, *Agric. For. Meteor.*, **39**, 205–223.

Kuwagata, T., H. Kanno, J. Asanuma, Y. Ma and X. Ma, 1999: Preliminary estimation of the daytime heating rate of the atmosphere over the Tibetan Plateau during '98 IOP using the diurnal variation of the surface pressure, *Third International Scientific Conference on the Global Energy and Water Cycle*, Beijing, China, 16–19 June 1999, 417.

Lhomme, J.-P., A. Chehbouni and B. Monteny, 1994: Effective parameters of surface energy balance in heterogeneous landscape, *Bound.-Layer Meteor.*, **71**(3), 297–310.

Li, Z.-L. and F. Becker, 1993: Feasibility of land surface temperature and emissivity determination from AVHRR data, *Remote Sens. Environ.*, **43**, 67–85.

Ma, Y., O. Tsukamoto, J. Wang, Z. Hu, H. Ishikawa, Z. Hu, I. Tamagawa and H. Gao, 1999a: The characteristics of micrometeorology in the northern Tibetan Plateau area, *Proceedings of the 1st International Workshop on GAME-Tibet*, Xi'an, China, 11–13 January 1999, 99–102.

———, J. Wang, M. Menenti and W. Bastiaanssen, 1999b: Estimation of fluxes over the heterogeneous land surface with the aid of satellite remote sensing and field observation, *ACTA Meteor. Sinica*, **57**, 180–189 (in Chinese with English abstract).

———, O. Tsukamoto, J. Wang, Z. Hu, H. Ishikawa, I. Tamagawa and H. Gao, 1999c: Transfer and micrometeorological characteristics in the surface layer of the atmosphere above Tibetan Plateau area, *Third International Scientific Conference on the Global Energy and Water Cycle*, Beijing, China, 16–19 June 1999, 55–56.

———, O. Tsukamoto, X. Wu, I. Tamagawa, J. Wang, H. Ishikawa, Z. Hu and H. Gao, 2000: Characteristics of energy transfer and micrometeorology in the surface layer of the atmosphere above marshland of the Tibetan Plateau area, *Chinese Journal of Atmospheric Sciences*, **24**(5), 715–722 (in Chinese with English abstract).

———, O. Tsukamoto, J. Wang, H. Ishikawa and I. Tamagawa, 2002a: Analysis of aerodynamic and thermodynamic parameters on the grassy marshland surface of Tibetan Plateau, *Progress in Natural Science*, **12**(1), 36–40.

———, O. Tsukamoto, H. Ishikawa, Zh. Su, M. Menenti, J. Wang and J. Wen, 2002b: Determination of Regional land surface heat flux densities over heterogeneous landscape of HEIFE Integrating satellite remote sensing with field observations, *J. Meteor. Soc. Japan*, **80**(3), 485–501.

Mason, P., 1988: The formation of areally averaged roughness lenghths, *Quart. J. Roy. Meteor. Soc.*, **114**, 399–420.

Menenti, M., W.G.M. Bastiaanssen, K. Hefny and M.H. Abd EI Karim, 1991: Mapping of ground water losses by evaporation in the Western Desert of Egypt, *DLO Winand Staring Centre, Report no. 43*, Wageningen, The Netherlands, 116pp.

——— and B.J. Choudhury, 1993: Parameteraization of land surface evaporation by means of location dependent potential evaporation and surface temperature range, in (eds.) Bolle, Feddes and Kalma, Exchange processes at the land surface for a range of space and time scales, IAHS Publ. No. 212, 561–568.

Monteith, J.L., 1965: Evaporation and environment, *XIXth Symposium, Soc. For Exp. Biol.*, Swansea, Cambridge University Press 1, 205–234.

Owen, P.R. and W.R. Thomson, 1963: Heat transfer across rough surface, *J. Fluid Mech.*, **15**, 321–334.

Paltridge, W. and Mitchell, M. Ross, 1990: Atmospheric and viewing angle correction of vegetation indices and grassland fuel moisture content derived from NOAA/AVHRR, *Remote Sens. Environ.*, **31**, 121–135.

Paulson, C.A., 1970: The mathematic representation of wind speed and temperature profiles in the unstable atmospheric surface layer, *J. Meteor. Soc. Japan*, **9**, 856–861.

Qi, J., A. Chehbouni, A.R. Huete, Y.H. Kerr and S. Sorooshian, 1994: A Modified Soil Adjusted Vegetation Index, *Remote Sens. Environ.*, **48**, 119–126.

Raupach, M.R., 1994: Simplified experissions for vegetation roughness length and zero-plane displacements as functions of canopy height

and area index, *Bound.-Layer Meteor.*, **71**, 211–216.

Sobrino, J.A. and N. Raissouni, 2000: Toward remote sensing methods for land cover dynamic monitoring, application to Morocco, *Int. J. of Remote Sensing*, **21**(2), 353–366.

Tamagawa, I., H. Ishikawa, O. Tsukamoto, T. Hayashi, S. Miyazaki, J. Asanuma, Y. Qi, H. Fudeyasu, K. Tanaka, Y. Ma, H. Gao and J. Wang, 1999: Preliminary analysis on the turbulent characteristics at Amdo PBL site on Tibetan Plateau, *Third International Scientific Conference on the Global Energy and Water Cycle*, Beijing, China, 16–19 June 1999, 413–414.

Tanaka, K., H. Ishikawa, T. Hayashi, I. Tamagawa and Y. Ma, 2001: Surface Energy Budget at Amdo on Tibetan Plateau using GAME/Tibet IOP'98 Data, *J. Meteor. Soc. Japan*, **79**(1B) GAME Special Issue, 505–517.

Taylor, P.A., R.I. Sykes and P.J. Mason, 1989: On the parameterization of drag over small scale topography in neutrally stratified Boundary flow, *Bound.-Layer Meteor.*, **48**, 409–422.

Tsukamoto, O., H. Fudeyasu, S. Miyazaki, K. Ueno, Y. Qi and Y. Ma, 1999: Turbulent surface flux measurements over Tibetan Plateau with flux-PAM system, *Third International Scientific Conference on the Global Energy and Water Cycle*, Beijing, China, 16–19 June 1999, 411–412.

Valiente, J.A., M. Nunez, E. Lopez-Baeza and J.F. Moreno, 1995: Narrow-band to broad-band conversion for Meteosat-visible channel and broad-band reflectance using both AVHRR-1 and -2 channels, *Int. J. Remote Sensing*, **16**(6), 1147–1166.

Valor, E. and V. Caselles, 1996: Mapping land surface emissivity from NDVI: application to European, African and South American areas, *Remote Sens. Environ.*, **57**, 167–184.

Wang, J., Y. Ma, M. Menenti and W. Bastiaanssen, 1995: The scaling-up of processes in the heterogeneous landscape of HEIFE with the aid of satellite remote sensing, *J. Meteor. Soc. Japan*, **73**(6), 1235–1244.

———, J. Kim, Y. Liou, Zh. Gao, Y. Yan, T. Choi and H. Lee, 1999: Energy balance analysis and one-dimensional simulation of land surface process in a short-grass site of Central Tibetan Plateau, *Third International Scientific Conference on the Global Energy and Water Cycle*, Beijing, China, 16–19 June 1999, 424–425.

Webb, E.K., 1970: Profile relationships: the log-liner range and extension to strong stability, *Quart. J. Roy. Meteor. Soc.*, **96**, 67–90.

Yasunari, T., 1999: Overview and highlights of the GAME-IOP, 1998, *Third International Scientific Conference on the Global Energy and Water Cycle*, Beijing, China, 16–19 June 1999, 402–403.